Research Inventy: International Journal of Engineering And Science
Vol.3, Issue 6 (August-2013), PP 63-76
Issn (e): 2278-4721, Issn (p):2319-6483, www.researchinventy.com

Optimal Design of A Simply Supported Composite Plate by Advanced Genetic Algorithm

Mr. Chakali Chandra Mohan[1], Mr. Karigi Sarath Chandra[2], Mr.Leelaramesh[3]
[1]*Professor, Department of Mechanical, Faculty of HITS, Hyderabad, India.*
[2]*Professor, Department of Mechanical, Faculty of HITS, Hyderabad, India.*
[3]*Asso. Professor, Department of Mechanical, Faculty of HITS, Hyderabad India.*

ABSTRACT: *The multi-objective optimization was carried out by first formulating separate weight and cost objective functions, and then forming a convex combination of the objectives. Compared to other multi-objective schemes, this method was simple to implement, requiring no additional modifications to the GA, since laminate fitness was still represented by a single value (i.e., by the combined cost and weight objective functions). However, results showed that this was not the most viable means of multi-objective optimization since it prevented the GA from finding the entire set of Pareto-optimal designs. This fault lies not with the GA, but with the fact that there is no convex combination of objective function values that will yield a Pareto-optimal point if the point does not lie on the Pareto-optimal curve, a phenomenon which occurred in this study. Nonetheless, further research is required to either improve on the ideas discussed in the paper, find better methods when using GAs for multi-objective optimization problems. The multi-objective scheme used in this work also required the scale factor to be adjusted in fine increments in order to obtain the set of Pareto-optimal designs for each loading condition, making this method somewhat computationally expensive.*
The purpose of this paper is to demonstrate the GA's ability to handle more complex composite optimization problems through simple modifications to the basic GA. These which discussed how to accommodate multiple materials in the stacking sequence. Further modifications, which are provided here, focus on the optimization formulation for such problems, and demonstrate one way of easily incorporating multiple objective functions into a genetic algorithm.

I. MULTI-OBJECTIVE OPTIMIZATION

The use of genetic algorithms for multi-objective optimization has been growing considerably in the past few years. GAs were originally used for maximization or minimization of an unconstrained function. However, there has been increasing interest in optimizing two or more criteria simultaneously, especially if it is difficult to represent one criteria in terms of another. These problems are often referred to as multi-objective (or vector-valued) optimizations problems. One such field of study utilizing this concept is the aerospace industry, where an effort has been made to incorporate cost directly into the design process. This methodology can lead to high performance designs that can be built with available materials and manufacturing techniques. Furthermore, such studies can be used to formulate trade off studies between cost and weight which may aid in the selection of a design that minimizes cost and/or weight [29], two of the most important considerations in aerospace applications.

The goal of single objective optimization problems is straightforward: find the maximum or minimum value of a function for a given set of parameters. The optimization concept is less clear for multi-objective problems, since the best value for one objective usually does not imply that the other objective(s) is simultaneously optimized. Thus, the concept of Pareto-optimality is often used in multi-objective problems to help determine the best way to simultaneously satisfy all objectives to the greatest extent possible.

Pareto-optimality can be explained by looking at a simple example where two generic objectives, P1 and P2 need to be minimized, and furthermore, it is difficult to estimate P1 in terms of P2 , or vice versa. (ˆP1 , ˆP2) is a Pareto optimum set if there is no other point (P1 ,P2) < (ˆP1 , ˆP2). In Figure 5.1, the relation between P1 and P2 is presented, showing five different points. Scenarios A, B, and C provide the best solutions to this problem, although neither one is best at minimizing both quantities at the same time (i.e., there is tradeoff in this problem since one quantity tends to increase as the other decreases). These three points (A,B,C) are referred to as Pareto-optimal (or non-dominated) [7] since no other point can generate lower values for both P1 and P2 simultaneously. The other options, D and E, are not Pareto-optimal (or are dominated) since C ¡ E and B ¡ D. Ultimately, the decision maker is left to decide which solution from the Pareto-optimal set is best. Many optimization studies have been aimed at optimizing two or more quantities simultaneously. The main difference between these studies is in the methodology for obtaining the Pareto-optimal curve. Kassapoglou [29] used multi-objective optimization to simultaneously minimize the cost and

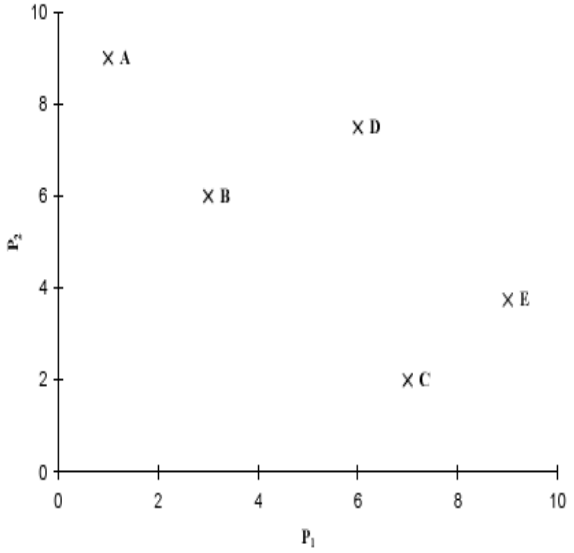

Figure 1: Multi-objective optimization.
The set {(P1 (x), P2 (x))} for 5 different design points.

weight of composite stiffened panels subjected to compression and shear loads. The first step in the optimization procedure involved minimizing each parameter separately. The lowest weight and cost configurations were then identified and placed in the Pareto-optimal set. Designs from the group optimized for cost that were lighter than the minimum cost configuration, and designs from the group optimized for weight that were cheaper to fabricate than the minimum weight configuration comprised the remainder of the candidate Pareto-optimal set. The optimum configuration from this set was chosen to be the one that minimized a certain penalty function. Although the individual minimum weight and cost designs did not coincide, results showed that a set of near-optimal designs could be found. Panels configured with "J" stiffeners provided the lowest weight, while "T" stiffeners produced the lowest cost designs and the best tradeoff between cost and weight.

Not surprisingly, GAs have also been applied to multi-objective problems. Schaffer [30] used genetic algorithms for multi-objective problems by creating equally sized sub-populations. Each sub-population worked on optimizing a single objective. Although selection was carried out in each sub-population individually, crossover was performed between members of both populations. Results showed that this implementation scheme was susceptible to bias against individuals that satisfied both objectives well but did not provide the optimum solution for either criteria, making it difficult to find the entire set of Pareto-optimal designs.

Belegundu et al. [31] implemented a GA in a slightly different manner for multi-objective optimization of a wide range of problems. The selection procedure in the GA was modified by replacing traditional roulette wheel selection with a scheme based on dominated and non-dominated designs. Designs that were non-dominated were given a rank of 1 while designs that were dominated or violated a constraint were given a rank of 2 and thrown away. Successive populations were made up of the parent designs (Rank 1) and a prescribed number of their offspring. If necessary, additional designs (referred to as immigrants) were randomly created to fill the remainder of the population, which also added diversity to the genetic search. This process continued until the entire population was filled entirely with non-dominated designs, the Pareto-optimal set. Preliminary testing of the GA showed that points on the Pareto curve were bunched into small groups instead of being spread out evenly, a phenomenon known as speciation [7]. This problem was handled by assigning twin or near twin designs a rank of two, thereby eliminating them from the Pareto set. Further testing of the algorithm showed that the GA was effective in generating Pareto solutions for optimizing aeromechanical responses for turbomachinery airfoils, and minimizing the cost and residual stresses in the fabrication of ceramic composite plates.

In this work, the multi-objective formulation will be carried out by applying a scale factor to cost and weight objective functions. To obtain a Pareto set of designs, the influence of cost and weight on the overall fitness of a plate configuration is adjusted from one extreme to the other by varying the scale factor accordingly. This allowed the general configuration of the GA to be maintained since the fitness of each laminate design is still based on a single value that is comprised of both cost and weight information. An indepth discussion of this methodology will be presented shortly.

II. PROBLEM FORMULATION

The composite panel under consideration is 36 in long, 30 in wide, and simply supported on all four sides, see Figure 5.2. The panel can be loaded under any combination of axial and shear loads (i.e., N_x, N_y, and N_{xy}). Each ply in the panel may be made of either graphite-epoxy or Kevlar-epoxy (see Table 5.1 for properties) and can have any ply orientation angle between -75^0 and 90^0, in Increments of 15°, as shown in Figure 5.2. The load handling capabilities of laminated composite plates comprised of two materials is the analysis used in this section of the paper. To determine these capabilities, two quantities must be found: the margin of safety for the critical buckling load, and the margin of safety for the principal ply strains.

2.1 Critical buckling load

To find the critical buckling loads for a symmetrically laminated anisotropic composite plate ($N_{x_{cr}}$, $N_{y_{cr}}$, $N_{xy_{cr}}$), the Galerkin energy method outlined in Whitney [32], was utilized. Realizing that there is no coupling between bending and extension for symmetric laminates (i.e., [Bij] = 0), the strain energy, U, for transverse bending of a laminated plate of length (x = a) and width (y = b) is

$$U = \frac{1}{2}\int_0^b \int_0^a \left[D_{11}\left(\frac{\partial^2 w}{\partial x^2}\right)^2 + 2D_{12}\frac{\partial^2 w}{\partial x^2}\frac{\partial^2 w}{\partial y^2} + D_{22}\left(\frac{\partial^2 w}{\partial y^2}\right)^2 + 4\left(D_{16}\frac{\partial^2 w}{\partial x^2} + D_{26}\frac{\partial^2 w}{\partial y^2}\right)\frac{\partial 2w}{\partial x \partial y} + 4D_{66}\left(\frac{\partial^2 w}{\partial x \partial y}\right)^2 \right] dxdy.,$$

where the bending stiffness' of the plate ([Dij]) are determined using classical lamination theory, see Jones [4]. Next, the potential energy, V, of the biaxial and shear loads ($N^a{}_y$, and $N^a{}_{xy}$) that are applied to the plate is considered

$$V = \frac{1}{2}\lambda \int_0^b \int_0^a \left[N_x^a \left(\frac{\partial w}{\partial x}\right)^2 + N_y^a \left(\frac{\partial w}{\partial y}\right)^2 + 2N_{xy}^a \left(\frac{\partial^2 w}{\partial x \partial y}\right) \right] dxdy.$$

To determine the governing equation for the composite plate, Hamilton's principle [33] is used

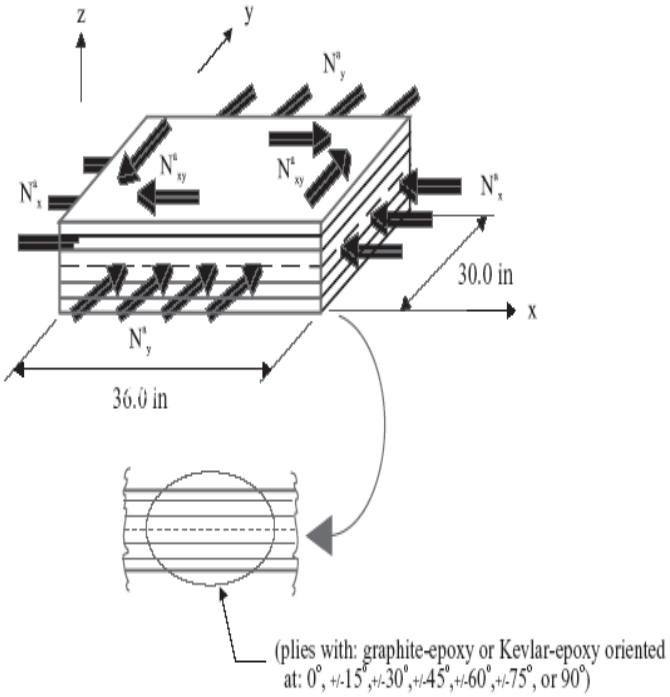

Figure.2: Configuration and loading conditions for simply supported plate.

Property	Gaphite-Epoxy	Kevlar-Epoxy
Young's modulus (longitudinal)	$E_{11} = 22.0 \times 10^6$ psi	$E_{11} = 11.9 \times 10^6$ psi
Young's modulus (transverse)	$E_{22} = 1.50 \times 10^6$ psi	$E_{22} = 0.6 \times 10^6$ psi
Shear modulus	$G_{12} = 0.52 \times 10^6$ psi	$G_{12} = 0.4 \times 10^6$ psi
Poisson's ratio	$\nu_{12} = 0.25$	$\nu_{12} = 0.25$
Ply thickness	$t = 0.00525$ in.	$t = 0.00716$ in.
Material density	$\rho = 0.0055 \frac{\text{lb}}{\text{in}^3}$	$\rho = 0.0048 \frac{\text{lb}}{\text{in}^3}$
Cost factor (per pound of material)	$C_f = 3.0$ /lb	$C_f = 1.0$ /lb
Allowable strain (longitudinal)	$\epsilon_{11}^{all} = 9.89 \times 10^{-3}$	$\epsilon_{11}^{all} = 2.87 \times 10^{-3}$
Allowable strain (transverse)	$\epsilon_{22}^{all} = 3.87 \times 10^{-3}$	$\epsilon_{22}^{all} = 3.00 \times 10^{-3}$
Allowable shear strain	$\gamma_{12}^{all} = 1.90 \times 10^{-3}$	$\gamma_{12}^{all} = 1.21 \times 10^{-3}$

$$- \int (-\delta U - \delta V) dt = 0,$$

where δU and δV are the first variations in strain energy and potential energy due to the in-plane loads, respectively. The governing equation for the composite plate takes the form of Table 6.1: Material properties for Kevlar/epoxy and graphite/ epoxy

$$\int_0^b \int_0^a \left[D_{11} \frac{\partial^4 w}{\partial x^4} + 2(D_{12} + 2D_{66}) \frac{\partial^4 w}{\partial x^2 \partial y^2} + 4\left(D_{16} \frac{\partial^4}{\partial x^3 \partial y} + D_{26} \frac{\partial^4 w}{\partial x \partial y^3} \right) \right.$$

$$\left. + D_{22} \frac{\partial^4 w}{\partial y^4} - \lambda \left(N_x^a \frac{\partial^2 w}{\partial x^2} - 2N_{xy}^a \frac{\partial^2 w}{\partial x \partial y} - N_y^a \frac{\partial^2 w}{\partial y^2} \right) \right] \delta w \, dx \, dy$$

$$+ 2 \oint_0^b \left[D_{26} \frac{\partial^2 w}{\partial x \partial y} \right] \frac{\partial(\delta w)}{\partial y} \, dx + 2 \oint_0^a \left[D_{16} \frac{\partial^2 w}{\partial x \partial y} \right] \frac{\partial(\delta w)}{\partial x} \, dy = 0.$$

Since the effects of the D_{16} and D_{26} terms are not neglected, the surface integrals in Eq. (6.4) are included in the governing equation. This allows the transverse deflection and first variation of the transverse deflection to be formulated in a double sine series

$$\sum_{m=1}^{M} \sum_{n=1}^{N} \left\{ \pi^4 \left[m^4 D_{11} + 2(D_{12} + 2D_{66})(mn)^2 + (nR)^4 D_{22} \right.\right.$$

$$\left. + \left(\frac{am}{\pi} \right)^2 \lambda N_x^a + \left(\frac{an}{\pi} \right)^2 \lambda N_y^a \right] A_{mn}$$

$$- 32mnR\pi^2 \left[\sum_{i=1}^{M} \sum_{j=1}^{N} M_{ij} (i^2 + m^2) D_{16} + R^2 (n^2 + j^2) D_{26} \right.$$

$$\left.\left. + \left(\frac{a}{\pi} \right)^2 \lambda N_{xy}^a \right] A_{ij} \right\} = 0, \quad \text{where}$$

$$M_{ij} = \begin{cases} \dfrac{ij}{(m^2 - i^2)(n^2 - j^2)} & (m \pm i) \text{ odd}, \quad (n \pm j) \text{ odd} \\ 0 & \text{otherwise}, \end{cases}$$

Substituting Eq. (6.5) into Eq. (6.4), performing the necessary integrations, and noting that the

$$w = \frac{\partial^2 w}{\partial x^2} = \frac{\partial^2 w}{\partial y^2} = 0 \qquad \text{(on the plate boundaries)},$$

following set of algebraic equations are obtained:

$$\begin{bmatrix} N_{x_{cr}} \\ N_{y_{cr}} \\ N_{xy_{cr}} \end{bmatrix} = \lambda_{cr} \begin{bmatrix} N_x^a \\ N_y^a \\ N_{xy}^a \end{bmatrix}. \qquad (5.8)$$

and R is defined as the plate aspect ratio (a/b). Equation (6.7) yields MN homogeneous equations that can be broken into the form of $[A]\{x\} - \lambda[B]\{x\} = 0$. The coefficient matrix, contains terms involving $N^a{}_y$, and $N^a{}_{xy}$ only. The smallest value of λ, λ_{cr}, for which the determinant of the coefficient matrix vanishes will give the values for the critical buckling loads Finally, λ_{cr} is used to calculate the margin of safety:

2.2 Principal ply strains

To complete the analysis, the margins of safety for the principle ply strains must be determined. The laminate strains for the composite plate are determined from the stress-strain relationship where the extensional stiffnesses, $[A_{ij}]$ are determined using classical lamination theory once again. To calculate the principal ply strains, the laminate strains are transformed through the ply angle θ using the methods described in Jones. The largest ratio of principal ply strain (ij) to the corresponding allowable strain (ij) is then used to calculate the margin of safety,

$$\begin{bmatrix} \epsilon_x \\ \epsilon_y \\ \gamma_{xy} \end{bmatrix} = \begin{bmatrix} A_{11} & A_{12} & A_{16} \\ A_{12} & A_{22} & A_{26} \\ A_{16} & A_{26} & A_{66} \end{bmatrix} \begin{bmatrix} N_x^a \\ N_y^a \\ N_{xy}^a \end{bmatrix}, \qquad (5.10)$$

$$\lambda_s = 1 - \max \left\{ \frac{\epsilon_{11}}{\epsilon_{11}^{all}}, \frac{\epsilon_{22}}{\epsilon_{22}^{all}}, \frac{\gamma_{12}}{\gamma_{12}^{all}} \right\}.$$

$$\begin{bmatrix} \epsilon_{11} \\ \epsilon_{22} \\ \gamma_{12} \end{bmatrix} = \begin{bmatrix} \cos^2\theta & \sin^2\theta & \sin\theta\cos\theta \\ \sin^2\theta & \cos^2\theta & -\sin\theta\cos\theta \\ -2\sin\theta\cos\theta & 2\sin\theta\cos\theta & \cos^2\theta - \sin^2\theta \end{bmatrix} \begin{bmatrix} \epsilon_x \\ \epsilon_y \\ \gamma_{xy} \end{bmatrix}.$$

The allowable strains for each direction (ε_{11}^{all}, ε_{22}^{all} and γ_{ij}^{all}) were determined by comparing maximum compressive and tensile values and choosing the smaller of the two (a conservative approach). The resulting values for each material are listed in Table 6.1

2.3 Optimization Procedure

The goal of the optimization is to find the stacking sequence of the plate which provides the lowest weight and cost but does not buckle or fail due to excessive strain. For simplicity, it is also assumed that the laminate stacking sequence is symmetric about the mid-plane and balanced. Since the GA works with a string that represents one half of the laminate stacking sequence, the symmetry constraint is automatically satisfied. The

balance constraint, which ensures that each ply oriented at $+\theta^\circ$ is complemented with another ply oriented at $-\theta^\circ$ throughout the stacking sequence, will be enforced using penalty parameters. Discussion of the optimization procedure is split into three sections: laminate weight and cost calculation, objective function formulation, and the formulation for multi-objective optimization.

III. CALCULATING LAMINATE WEIGHT AND COST

The panel weight is calculated as

$$W = ab[\rho_{ke} t_{ke} N_{ke} + \rho_{ge} t_{ge} N_{ge}]$$

where a and b are the dimensions of the plate, ρ_{ke} and ρ_{ge} are the material densities, t_{ke} and t_{ge} are the corresponding ply thicknesses for each material, and N_{ke} and N_{ge} are the number of plies of Kevlar-epoxy and graphite-epoxy in the laminate stacking sequence, respectively.

The cost of a laminate is based on two quantities: material cost and lay-up cost. The material cost for a laminate, C_m, is determined by multiplying the weight of each material in a laminate by its corresponding cost factor (C_f) given in Table 6.1:

$$C_m = ab[C_{f_{ke}} \rho_{ke} t_{ke} N_{ke} + C_{f_{ge}} \rho_{ge} t_{ge} N_{ge}].$$

Lay-up cost, C_l, is based on the amount of time required by the lay-up machine to construct each laminate. Data was obtained from a standardized manufacturing process relating ply orientation angle and plate dimensions. However, since the dimensions of the plate are the same for each laminate, lay-up cost becomes a function of ply orientation angle only.

The analysis procedure used to compute the layup cost can not be revealed in this document because they are company proprietary information. Instead, we have given a table which shows a multiplier for the layup cost as a function of the ply orientation angle (the table is coded into the algorithm to provide information on layup cost when needed). This information, depicted in Figure 3, shows that the most expensive plies to construct are those oriented at $\pm 45^\circ$. Plies oriented at 0° degrees are more expensive than 90° plies because the plate is 6 inches longer in the x direction. The total cost for a laminate can now be determined by adding the corresponding material and lay-up costs:

$$C_t = C_m + C_l.$$

3.1 Objective Function Formulation

The optimization problem can be formulated as:
minimize W and C_t such that

$$\lambda_b, \lambda_s \geq 0, \qquad (6.16)$$

where λ_b and λ_s are the margins of safety for the critical buckling load and principal ply strains, respectively. Two fitness functions will be utilized for this problem, one for laminate weight (Φ_W) and another for laminate cost (Φ_C). To accommodate the genetic algorithm, the degree of constraint

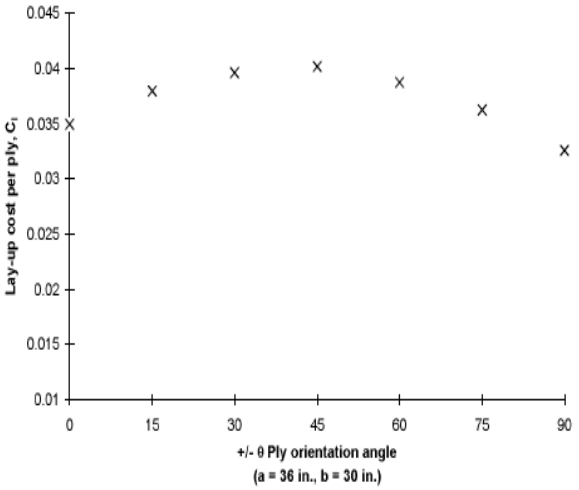

Figure.3: Lay-up costs for different ply orientation angles.

violation or satisfaction must be transformed into added penalties or bonuses [18] that augment each objective function.

The fitness function for laminate weight is defined by

$$\Phi_w = \begin{cases} W + P_{ke}^w + P_{ge}^w - \epsilon_r^w, & \text{feasible laminates,} \\ W\epsilon_p + P_{ke}^w + P_{ge}^w, & \text{infeasible laminates.} \end{cases} \tag{5.17}$$

$$P_x^w = \begin{cases} 0, & \text{laminate balanced,} \\ N_{ub_x} w_x, & \text{laminates unbalanced,} \end{cases} \tag{5.18}$$

$$\epsilon_r^w = w_a \min\{\lambda_b, \lambda_s\}, \tag{5.19}$$

Since the first objective is weight minimization, the numerical values of the bonus and penalty parameters given in Eq. 6.17, which will be discussed in the following paragraphs, are proportional to the ply weights of each material, providing a means of penalizing or rewarding a laminate by adjusting laminate weight. For example, if a laminate violates a constraint, a penalty parameter is added to the weight, W, making the laminate less desirable because its weight has been artificially increased. To enforce the balance constraint for both materials, two penalty parameters, P^{w}_{ke} and P^{w}_{ge}, are added to the objective function where w is the weight of a single ply, N_{ub} is the number of unbalanced plies in the laminate, and x = ke, ge for Kevlar-epoxy and graphite-epoxy, respectively. Thus, if either material has unbalanced plies in a laminate, the laminate is penalized by an amount equal to the weight of the number of unbalanced plies, making the laminate artificially heavier and thereby less desirable.

The formula for feasible laminates in Eq 17 is used if all constraints are satisfied. Feasible laminates are rewarded with a bonus, ε_r^w, whose value depends on the average material weight of a ply, and the amount of constraint satisfaction so that designs satisfying the constraints by a larger margin become more desirable. The constraint that is closest to being violated is used to calculate the bonus parameter:

where w_a represents the average weight of a ply.

If a constraint is violated the formula for infeasible laminates shown in Eq. 6.17 is used. A laminate is artificially made heavier using the penalty parameter, p:

$$\square_p = (1 - \min\{\lambda_b, \lambda_s\})^P. \tag{6.20}$$

The penalty parameter is rationalized by first using a scale factor determined by the value of the most violated constraint. Laminates that are very thin may appear desirable even when a constraint is violated. This problem is handled by adding the exponent P to the scale factor. A value for P will be determined in the multi-objective formulation given in the next section. Parameters $\square^{w}_{r}$ and $\square_p$ are used only if all constraints are satisfied or at least one constraint is violated, respectively.

The objective function for laminate cost is formulated in a manner similar to the one for weight, except that bonus and penalty parameters are now proportional to the material and lay-up costs for a ply:

$$\Phi_c = \begin{cases} C_t + P_{ke}^c + P_{ge}^c - \epsilon_r^c, & \text{feasible laminates,} \\ C_t\epsilon_p + P_{ke}^c + P_{ge}^c, & \text{infeasible laminates.} \end{cases} \tag{5.21}$$

The balance constraints were modified first

$$P_x^c = \begin{cases} 0, & \text{(laminate balanced)}, \\ N_{ub_x}(c_a^l + c_x^m), & \text{(laminates unbalanced)}, \end{cases} \tag{5.22}$$

where c^l_x is the cost for a single ply of material x = ke, ge for Kevlar-epoxy and graphite-epoxy, respectively. The parameter c^l_a is determined by dividing the sum of the lay-up costs for each permissible ply orientation angle, c^l_i, by the total number of permissible angles, N_{pa}:

$$c_a^l = \frac{\sum_{i=0°,15°,30°\ldots}^{90°} c_i^l}{N_{pa}}. \tag{5.23}$$

Next, the bonus parameter, c_r was developed to make feasible laminates artificially appear less expensive and thus more desirable:

$$\epsilon_r^c = (c_a^l + c_a^m)\min\{\lambda_b, \lambda_s\}, \tag{5.24}$$

where c^m_a is the average material cost of a single ply. The parameter used to penalize infeasible laminates, p is identical to the one used for the weight objective function, see Eq. 20.

3.2 Multi-Objective Formulation

The multi-objective formulation is carried out by using a convex combination of the weight and cost objective functions determined in the previous section. This allows the fitness of each laminate to be represented by a single quantity:

$$\Phi_{lam} = \alpha c + (1 - \alpha) w, \qquad 0 \le \alpha \le 1.$$

By combining Eq. 5.17 and Eq. 5.21, a more detailed expression can be obtained

$$\Phi_{lam} = \begin{cases} \left[W + P_{ke}^w + P_{ge}^w - w_a M\right](1-\alpha) + \\ \left[C_t + P_{ke}^c + P_{ge}^c - (c_a^l + c_a^m)M\right]\alpha, & \text{feasible laminates}, \\ \left[W(1-M)^P + P_{ke}^w + P_{ge}^w\right](1-\alpha) + \\ \left[C_t(1-M)^P + P_{ke}^c + P_{ge}^c\right]\alpha, & \text{infeasible laminates}, \end{cases} \tag{5.26}$$

where $M = \min\{\lambda_b, \lambda_s\}$. A set of Pareto optimal designs can be determined by varying α in small increments from zero to one. To complete the formulation, the GA was tested to determine a value for P. Initial results using a value of P = 1 showed that thin laminates which violated a constraint were more desirable than feasible laminates. Further testing showed that increasing P to a value of 2.7 eliminated this problem without penalizing feasible laminates too much.

IV. RESULTS

Results will be given in two subsections. The first subsection will consider results obtained for uniaxial loading conditions, and the second subsection will consider results for biaxial loading. For these load cases, the value of α was varied from 0 to 1 in increments of 0.01, yielding 101 different combinations of cost and weight in the objective function. Fifty optimization runs, using a population size of fifty for each run, were conducted for each value of α. The best design from each set of runs is placed in the Pareto-optimal set. Using this approach, there is a possibility for different values of α to yield the same optimal design due to the discrete nature of the problem. But since the finite number of Pareto-optimal designs is unknown, many values for α were used to improve the chances of finding the entire set. For all runs conducted GA operator probabilities are listed in Table 6.2.

4.1 Uniaxial Loading

Operator	Probability
Crossover	1.00
Single ply alteration (orientation)	0.05
Single ply alteration (material)	0.05
Ply addition	0.05
Ply deletion	0.10
Permutation	0.75

Table 2: GA operator implementation probabilities

In this section, the laminated plate was placed under a compressive load of 100 lbs/in along the x– axis of the plate, see Figure 1.4. For this configuration, 6 designs were found in the Pareto-optimal set. The GA was successful in finding only five of these designs, see Figure 6.5. Point A depicts the minimum weight design while point F is the lowest cost design. Design D, represented by an "×" in Figure 1.5, could not be found by the GA for any of the values of α used. The reasons for this will be explained shortly.

The properties of each design are given in Table 6.3 and Table 6.4 (the strain constraint was not critical and is not listed). The stacking sequence representation gives the ply orientation angles and material makeup for one half of the symmetrically laminated plate, with the left end corresponding to the outer edge. In the discussion of the various laminate designs that follow, references will be made to the left half of the laminated stacking sequence only. Plies that are made from graphite are superscripted with a (1), while those made from Kevlar are superscripted with a (2).

As seen in Table 6.3, the possibility for different values of α yielding the same design was realized for this problem. Since numeric values for cost are considerably larger than those for weight, many of the different designs were found for small values of α, where the objective function for laminate weight had sufficient influence on the overall fitness of a laminate. The small number of designs found by the GA is due to the discrete nature of the problem. Unlike continuous optimization

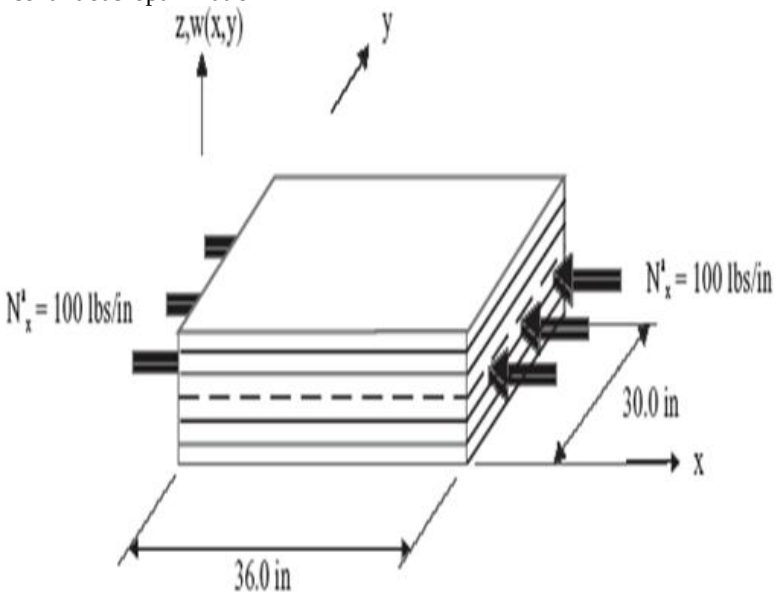

Figure 4: Plate configuration: uniaxial loading.

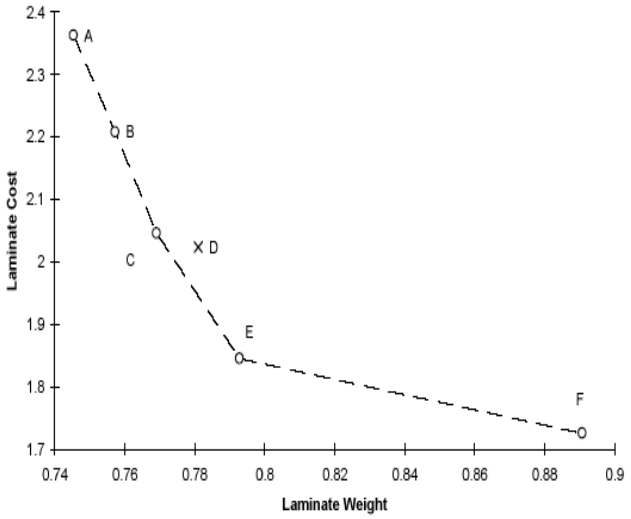

Figure 5: Set of Pareto-optimal designs for uniaxial loading.

problems, an infinite number of possibilities for laminate weight and cost do not exist between point A and point E. The set of optimal laminate designs for this problem are comprised of either 11 or 12 plies. Any design consisting of 10 plies violates the critical buckling load constraint, regardless of stacking sequence or material type arrangement. All laminate comprised of 13 or more plies are dominated, in a Pareto sense, by other designs.

Design	Stacking sequence	Thickness	No. of plies	α
A	$[\pm 45_3^{(1)}/\pm 45_2^{(2)}/90^{(2)}]_s$	0.1346in	11	0.00, 0.01, 0.02
B	$[\pm 45_2^{(1)}/90^{(1)}/\pm 60_2^{(2)}/90_2^{(2)}]_s$	0.1384in	11	0.03, 0.04,...,0.06
C	$[\pm 45_2^{(1)}/90_7^{(2)}]_s$	0.1422in	22	0.07, 0.08,...,0.10
D	$[\pm 45^{(1)}/90^{(1)}/\pm 45_4^{(2)}]_s$	0.1461in	11	not found
E	$[\pm 45^{(1)}/\pm 45^{(2)}/\pm 60^{(2)}/90_5^{(2)}]_s$	0.1499in	11	0.11, 0.12,...,0.40
F	$[30^{(2)}/60^{(2)}/-30^{(2)}/-60^{(2)}/90_8^{(2)}]_s$	0.1718in	12	0.41, 0.42,...,1.00

Once the minimum number of plies for a laminate is determined, the only way for the GA to obtain the Pareto-set of designs is to adjust a ply's material type or its orientation angle, both of which offer a discrete set of choices. Although there are numerous designs with different values for cost, there are very few choices when trying to find laminates with different weight. This is because weight can only be adjusted by altering a ply's material type or shifting between 11 or 12 plies. On the other hand, the cost of a laminate can be adjusted in many ways by using different ply orientation angles (in addition to switching material types and the number of plies). Thus, the number of designs in the Pareto-set is governed by the few available choices for laminate weight. Design A represents the lightest laminate. Since the critical buckling load is the active constraint, the GA chose a combination of plies from both materials that yields the lightest laminate with the highest bending stiffness. For this problem, high bending stiffness was achieved by using a combination of high strength material, orienting plies at 45°, and increasing the laminate thickness as much as possible. Since plies that are furthest from the laminate mid-plane have the most influence on a laminate's bending stiffness, the GA found a design with six $\pm 45^\circ$ plies of high strength graphite-epoxy at the outer edges of the laminate. The inner portion of the laminate is comprised of Kevlar-epoxy plies, four oriented at $\pm 45^\circ$ and one oriented at 90° to satisfy the balanced constraint. Although lower in strength, each ply of Kevlar is over 35% thicker than a ply of graphite. By using thicker plies, the graphite material is pushed further away from the

Table : Laminate properties for Pareto-optimal designs, uniaxial loading.

Design	Weight	Layup cost	Material Cost	Total Cost	Buckling Load
A	0.7454	0.8686	1.4938	2.3624	99.32 lbs/in
B	0.7573	0.8270	1.3810	2.2080	99.94 lbs/in
C	0.7691	0.7776	1.2681	2.0457	100.06 lbs/in
D	0.7810	0.8686	1.1552	2.0238	100.63 lbs/in
E	0.7929	0.8023	1.0423	1.8446	101.404 lbs/in
F	0.8908	0.8350	0.8908	1.7258	100.72bs/in

otherwise be achieved by using graphite-epoxy throughout the stacking sequence, and provides the maximum bending stiffness.

If the GA were to use all graphite-epoxy plies, the lowest weight design that does not buckle would be $[\pm 45^{(1)}{}_6 /90^{(1)}]_S$, requiring two additional plies to satisfy the buckling constraint, an increase of over 4% in weight when compared to design A. Since graphite plies are thinner, more of them are required to provide the necessary laminate thickness to prevent buckling. Likewise, if Kevlar- epoxy were used throughout the stacking sequence, the lightest laminate would consist of 12 plies. This design is 19.5% heavier than A, requiring more material to satisfy the buckling constraint since Kevlar is not as strong as graphite. Thus, to find the lightest design, the GA found a design comprised of plies which provided the correct balance of high strength material and laminate thickness in the stacking sequence.

Point B represents the second lightest design in the Pareto set. Although cheaper to fabricate, this design is also slightly heavier than design A. Material cost is reduced by trading two plies of graphite for Kevlar. Since the GA works with only half of the laminate stacking sequence, this results in an odd number of graphite plies, one oriented at 90° to satisfy the balanced constraint. Layup cost is decreased by switching 2 stacks of $\pm 45^\circ$ plies to a stack of $\pm 60^\circ$ and two plies oriented at 90°. Although there is a smaller amount of graphite in the stacking sequence, and fewer plies that are oriented at $\pm 45^\circ$, there is sufficient increase in laminate thickness to satisfy the buckling constraint. The end result is an increase in weight of approximately 1.6% and a savings of over 6.5% in laminate cost, with almost no change in the critical buckling load.

As laminate cost becomes more influential in the optimization process, the GA searches for ways to satisfy the buckling constraint while using plies of less expensive Kevlar. Furthermore, the GA must find designs with fewer $\pm 45^\circ$ plies in the stacking sequence since they are more expensive to layup. The GA responds by once again changing a single ply of graphite to Kevlar, which increases laminate thickness and reduces material cost. Of all graphite plies, the one oriented at 90° is changed because it has the smallest effect on laminate bending stiffness due to it is orientation angle and its distance from the mid-plane. Switching the 90° ply does not disturb the balanced constraint either. The remaining plies of Kevlar are also oriented at 90°, minimizing laminate cost but still providing enough thickness to prevent buckling. This modification reduces the overall cost of the laminate by over 7.5% when compared to design B.

The stacking sequence for design E is influenced mostly by the cost of the laminate. Thus, the GA eliminates all but two plies of graphite-epoxy. With less graphite in the laminate, the buckling constraint is satisfied because thickness is increased and plies are oriented at angles which give the most bending stiffness (i.e., $\pm 45^\circ$ and $\pm 60^\circ$). Once again, plies furthest from the mid-plane are oriented at $\pm 45^\circ$ to satisfy the buckling constraint.

In finding designs A, B, and C in the Pareto set, the GA gradually increased laminate weight by trading one ply of graphite for Kevlar in each successive step. However, the weight increase from design C to E resulted from changing two plies of graphite to Kevlar. Thus, it was of interest to see if there was a design, comprised of three plies of graphite and eight plies of Kevlar, that would provide weight and cost characteristics between those of designs C and E. To see if the GA could find this design, α was varied between 0.10 (the value of α which produced design C) and 0.11 (which produced design E), in increments of 0.001. Although fifty optimization runs were conducted for each refined value of α, the GA could still not find design D. Thus, design D is represented with an "×" in Figure 1.5

However, by manually adjusting the ply orientation angles using three plies of graphite (placed at the outer edge)

and eight plies of Kevlar, design D was quickly located. The reason that the GA could not find this design can be explained by looking at the fitness values for designs C, D, and E for each value of $0.1 < \alpha < 0.11$. This data, listed in Figure 5.6, shows that design C is the most attractive design initially. As α increases, the fitness value for design E becomes smaller than design C's, while design D's fitness value is substantially higher than these two, regardless of the value for α. Although design D's fitness may eventually become more attractive than design C, it will never simultaneous be smaller than both D and E, making it impossible for the GA to find it. A possible explanation of this phenomenon is given by Das and Dennis [43] who argue that using convex combinations of objective functions will not produce the entire set of Pareto-optimal points if the Pareto-optimal curve is not convex. It can be seen in Figure 5.5 that design D clearly makes the Pareto curve non-convex.

For design F, cost is the only consideration in the optimization process. Thus, to achieve the lowest possible material cost the GA uses only Kevlar in the stacking sequence. Since Kevlar is not strong as graphite, 12 plies are required in the stacking sequence to satisfy the buckling constraint (as opposed to 11 for all other designs). To reduce layup cost as much as possible the stacking sequence consists of eight plies oriented at 90°. The remainder of the laminate is made up plies oriented at $\pm 30^\circ$ and $\pm 60^\circ$ and are placed at the outer edges of the laminate. This configuration reduces layup cost as much as possible put produces enough bending stiffness to satisfy the buckling constraint. Although a large jump in laminate weight exists between points E and F, designs found between these two points were either dominated, or violated the buckling constraint.

The general buckling mode shape for all designs in the Pareto set is shown in Figure 1. Under uniaxial loading conditions, the plate deforms in the shape of one half sine wave in both the x and y directions.

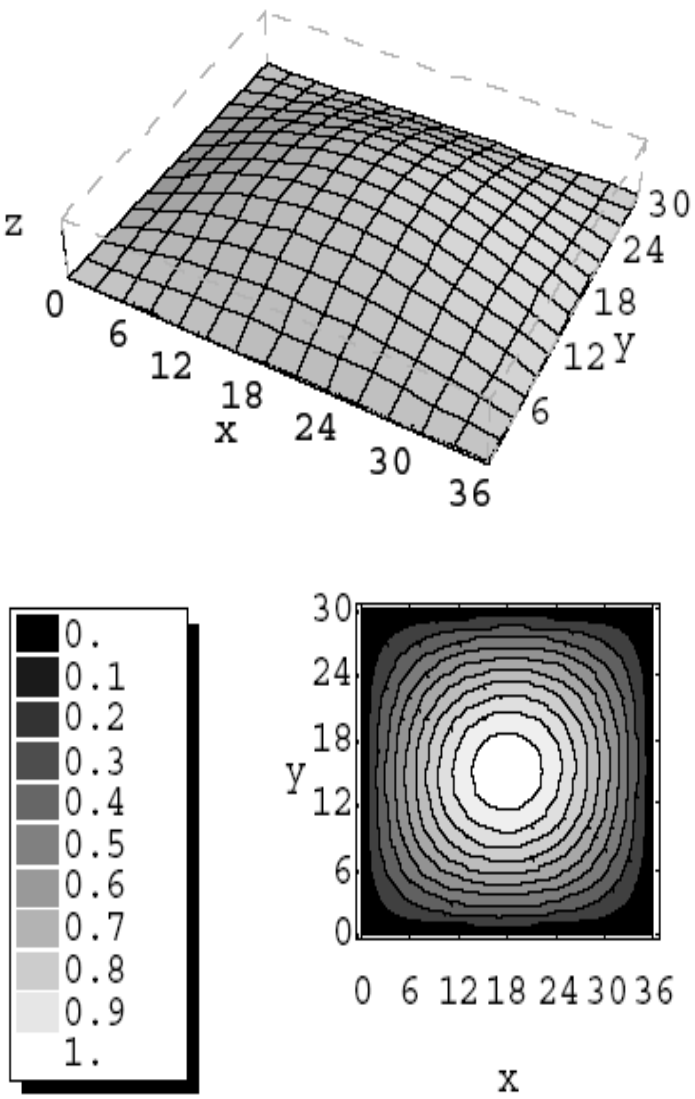

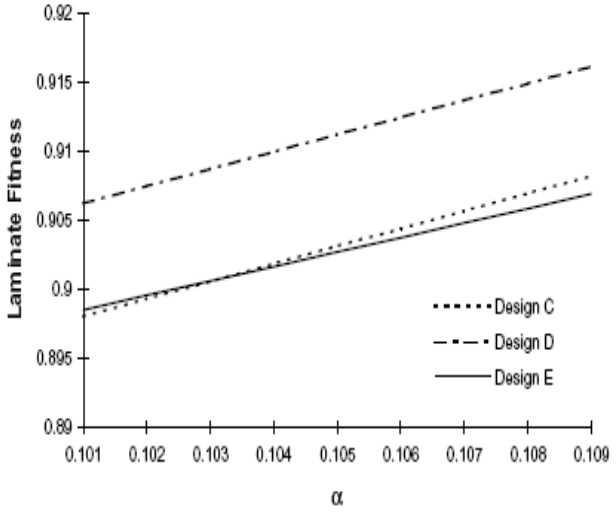

Figure: Fitness comparison between designs C, D, and E for specific values of α.

4.2 Biaxial Loading

In this section, results are reviewed for biaxial loading conditions, see Figure 6.8. A discrete set of Pareto-optimal points, consisting of 9 designs was found for this case, see Figure 1.9. Laminate properties for all designs are listed in Table 6.5 and Table 6.6. The GA used similar techniques discussed in the previous section to find this set of designs. To begin with, the GA finds the combination of graphite and Kevlar that yield the lowest possible number of plies. For design G, the lightest design, the minimum number of plies required to satisfy the buckling constraint (the strain constrain was inactive once again) is 15, 8 plies of graphite and 7 plies of Kevlar. As cost is gradually added to the objective function, the GA replaces graphite with Kevlar and finds stacking sequences that are less expensive to layup but still provide enough bending stiffness to prevent the laminate from buckling. The cheapest design, O, is made entirely of Kevlar and is comprised of 16 plies.

Points J, L, and N represent designs that were not found by the GA for any value of α during the initial set of runs conducted, and are listed in bold in Table 5.5 and Table 5.6. Once again, these designs contained a combination of materials that yielded a value for laminate weight between designs previously found by the GA. For example, since design I contains six plies of graphite and design K contains four plies of graphite, it seemed likely that there may be a design between these two which may fit into the Pareto set (i.e., design J, which contains five plies of graphite). Similar scenarios existed for designs L and N also.

To see if the GA could locate these designs, steps utilized in the previous subsection (for locating design D) were used again for this problem. For design J, α was varied between 0.09 (which pro-

Figure 8: Plate configuration: biaxial loading.

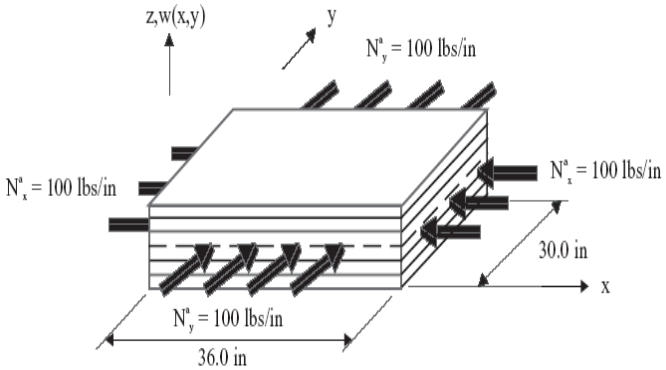

duced design I) and 0.1 (which produced design K) in increments of 0.001 For designs L and N, α was varied between 0.10 and 0.11, and 0.44 and 0.45, respectively. Although the GA was able to locate design J (repesented by a "2" in Figure 5.9) for α = 0.092, 0.093, it was unable to find designs L or N. Figure 10 shows that varying α between 0.10 to 0.11, the fitness value for design M becomes more attractive than design K, while design L's fitness is substantially higher than both of these during the transition. Similarly, the fitness of design N is never simultaneously lower than values attained for designs M or O, see Figure 11. In addition, by

looking at Figure 5.9, designs L and N make the Pareto-optimal curve non-convex, supporting the claim made by Das and Dennis [43] that such design points cannot be found with a convex combination of objective functions. Thus, it was impossible for the GA to find these designs which are represented with an "×" in Figure 9.

Design	Weight	Layup cost	Material Cost	Total Cost	Buckling Load
G	1.0186	1.0821	2.0165	3.0986	100.29 lbs/in
H	1.0305	1.0574	1.9037	2.9611	100.34 lbs/in
I	1.0423	1.0518	1.7908	2.8426	102.09 lbs/in
J	**1.0542**	**1.0383**	**1.6779**	**2.7162**	**100.30 lbs/in**
K	1.0661	1.0327	1.5650	2.5977	100.39 lbs/in
L	**1.0779**	**1.0574**	**1.4521**	**2.5096**	**99.95 lbs/in**
M	1.0898	1.0574	1.3393	2.3967	100.03 lbs/in
N	**1.1759**	**1.0731**	**1.3006**	**2.3738**	**100.64 lbs/in**
O	1.1878	1.0923	1.1878	2.2800	102.42 lbs/in

The general buckling mode shape for the entire set of Pareto-optimal designs found for biaxial loading are shown in Figure 12. Once again, the plate deforms into a half sine wave in both the x and y directions.

REFERENCES

[1]. Callahan, K. J., and Weeks, G. E., "Optimum Design of Composite Laminates Using Genetic Algorithm." Composite Engineering, Vol. 2, No. 3, 1992, pp. 149-160.

[2]. Nagendra, S., Haftka, R. T., and Gurdal, Z.,"Design of Blade Stiffened Composite Panels by a Genetic Algorithm." Proceedings of the 34th Structures, Structural Dynamics, and Materials Conference, La Jolla, CA, April 19-21, 1993, pp. 2418-2436.

[3]. Nagendra, S., "Optimal Stacking Sequence Design of Stiffened Composite Panels with Cutouts." Ph.D. Dissertation, Virginia Polytechnic Institute and State University, June 1993.

[4]. Nagendra, S., Jestin, D., G¨urdal, Z., and Watson, L. T., "Improved Genetic Algorithm for the Design of Sti_ened Composite Panels." Computers & Structures, Vol. 58, No. 3, 1996, pp. 543-555

[5]. Orvosh D. and Davis L., "Shall We Repair? Genetic Algorithms, Combinatorial Optimization, and Feasibility Constraints." Proceedings of the 5th International Conference on Genetic Algorithms, University of Illinois at Urbana-Champaign, Morgan Kaufmann Publishers, 1993, pp. 650.

[6]. Nagendra, S., Haftka, R. T., and G¨urdal, Z., "Stacking Sequence Optimization of Simply Supported Laminates with Stability and Strain Constraints. " AIAA Journal,Vol. 30, No. 8, 1992, pp. 2132{2137.

[7]. Mesquita, L., and Karmat, M. P., "Optimization of Sti_ened Laminated Composite Plates with Frequency Constraints." Engineering Optimization, Vol. 11, 1987, pp. 77-86.

[8]. Hajela, P., "Genetic Search - An Approach to the Non-convex Optimization Problem." AIAA Journal, Vol 28, No. 7, 1990, pp. 1205-1210.

[9]. Rao, S. S., Pan, T. S., and Venkayya, V. B., "Optimal Placement of Actuators in Actively Controlled Structures Using Genetic Algorithms." AIAA Journal, Vol. 29, No. 6, 1990, pp. 942-943.